New York Metro-Area Boundary Layer Catalogue: Boundary Layer Height and Stability Conditions from Long-Term Observations

Melecio-Vazquez, D.**; Gonzalez-Cruz, J.; Arend, M.; Han, Z.; Gutierrez, E.; Dempsey, M.; Booth, J.
The City College of New York , 160 Convent Ave., New York, NY, USA
***dmeleci00@citymail.cuny.edu*

1. Abstract

The focus of this paper is to highlight the findings from an observational analysis of wind, temperature, and relative humidity vertical profiles for the estimation of hourly stability conditions and the seasonal trends in boundary layer heights in the very dense city of New York. A microwave radiometer and a RADAR wind profiler jointly measured the measured thermal and momentum conditions for the determination of the seasonal diurnal cycle averages. The measured values cover a period from 2010 to 2014. A local static stability definition based on the vertical gradient of the virtual potential temperature is used which is then averaged to 500m for hourly reports of the static stability. Planetary boundary layer (PBL) heights were estimated from two methods that consider the potential temperature gradient, and the relative humidity gradient. Comparison of the summer static stability conditions are compared to the static stability calculated from a heat wave event that occurred on July 17-19 2013. Boundary layer heights show seasonal trends in line with observations conducted in the city of Oakland, CA using the same two methods.

2. Introduction

As populations in cities are expected to increase worldwide in the upcoming years (Department of Economic and Social Affairs, 2014), the climate in urban centers are receiving an increased focus in atmospheric and climate research. This increase in scientific activity may lead to further development of building and facilities that in turn will impact local weather. Studies have been made in observing the effect of urban centers in storm modification (Niyogi et al. 2011), and in their modification to local temperatures through what is known as the urban heat island (Oke 1988; Gedzelman et al. 2003) effect. Mesoscale models such as the Weather Research and Forecasting (WRF) model, have been implementing urban schemes that seek to simulate the complicated land-use and atmospheric interactions present within cities (Chen et al. 2011; Martilli et al. 2002, Tibana et al. 2014).

The focus of this analysis is to document observations of the vertical structure of atmospheric variables such as temperature, wind, and humidity in the very complex urban environment of New York City. It is in this topic that the use of remote sensing instruments have played a major role in urban climate research. A recent publication summarizes the current state of these technologies and some of the “long-term” (i.e. more than a month) studies on wind and turbulence profile measurements in various cities (Emeis 2011). The two technologies relied upon for the present analysis is a microwave and radiometer (MWR; for temperature and humidity) and a Doppler radar wind profiler (RWP; for wind speed and wind direction).

From the thermal and moisture profiles of the MWR, the atmospheric conditions will be categorized according to static stability. In general, the stability of a flow is characterized by its ability to restrict the growth of small perturbations. Static stability in particular focuses on the effect of the buoyancy to encourage/inhibit motion after a parcel of air has been perturbed (Stull 1991). Furthermore the static stability can be determined solely from the profile of the virtual potential temperature (Stull 1988). In this study the vertical gradient of the virtual potential temperature, $\partial\theta_v/\partial z$, will be used as a direct proxy for the static stability in both its sense (positive or negative) and magnitude, in a local sense (Arya 2008).

The planetary boundary layer height is another key variable that is used in defining the state of the atmosphere and is especially relevant to air pollution studies. Studies ranging from the use of remote sensing equipment (ie. Cohn and Angevine 2000) and numerical modeling (ie. Schmid and Niyogi 2012) have been used to estimate this very important height. The focus on boundary layer heights is solely on trends seen from heights derived from the thermal profiles of the atmosphere. Two methods derived from a study of radiosonde profiles were chosen for this study (a potential temperature method and a relative humidity method) and results show comparable trends in seasonal variation of Oakland, CA (methods and Oakland results can be found in Seidel et al. 2010).

In this study two instruments located in the region of the New York-New Jersey metropolitan region are used to produce diurnal climatologies for each season. A short review of the instrumentation is provided followed by data availability. Next, the method used to determine the static stability for each hour is defined
Discussion in the literature regarding the proper definition for the static stability is generally split between a local and nonlocal approach. Both of them are discussed in (Arya 2008). Although a thorough discussion of these distinctions is outside of the scope of this paper, the main concern in convective environments is that a local approach may label the mixing layer as a neutral layer, thus missing the instability present in that portion of the

atmosphere. Keeping this in mind the local approach is nevertheless utilized and the diurnal average of the data is compared against the July 2013 heat wave for comparison.

3. Observational Data

3.1 Instrumentation

The instruments used in this analysis are the Radiometrics Profiling Radiometer model MP-3000A and the Vaisala LAP-3000 Wind Profiler. Figure 1 shows the location of these instruments within the urban makeup of the New York-New Jersey Metropolitan region. The instruments are located about 15 km away from each other with the MWR located at the roof of the engineering building at the City College of New York (40.821519°,-73.948184°), and the wind profiler located at a roof at the Liberty Science Center in Jersey City (40.708009°, -74.054778°).

The MWR is a passive instrument that measures the vertical profiles of the temperature, the relative humidity, water vapor density and the liquid water density up to a height of 9800m AIL. It operates at a frequency range of 22 to 59 GHZ with a temperature resolution of 0.1 K to 1 K. The instrument also provides “surface” values which are measured from within the casing of the instrument and thus do not represent the actual surface temperature and were discarded from the analysis. The first level starts at a height of above 100 m AIL; the height above sea-level for the instrument is about 65 m. Further information on the instrument may be found at: http://srt-wp4.oa-cagliari.inaf.it/MYDATA/public_data/reports/radiometro/ MP_Specifications_7-3-07.pdf.

The wind profiler is an active instrument that measures the wind speed and wind direction of aerosols in the atmosphere. It is assumed that these aerosols are in equilibrium with the wind and thus also represent the local wind dynamics. The instrument operates at a frequency of 915 MHz with a wind speed accuracy <1 m/s and wind direction accuracy of <10 degrees. The vertical limit of this instrument is <2200 m and thus limits the concurrent investigation of the thermal and momentum structure of the atmosphere to this range. In addition to the wind speed and wind direction products, the signal-to-noise ratio and other beam characteristics are also measured but were not used directly in this study. Further information on the instrument may be found at: http://ghrc.nsstc.nasa.gov/uso/ds_docs/gpmgv/gcpex/gpmwpecgcpex/lap-3000_brochure.pdf.

Figure 1: Location of observing instruments in the New York-New Jersey Metropolitan Area. The microwave radiometer (MWR) is located in the northern part of Manhattan island (40.821519°,-73.948184°). The radar wind profiler (RWP) is located at the Liberty Science Center in Jersey City, New Jersey (40.708009°, -74.054778°).

3.2 Data Availability

Inherent in any observational effort done to characterize the atmosphere is the question of data availability. The days for which data is available from the microwave radiometer, wind profiler, and concurrent days of microwave radiometer and wind profiler measurement are given in Figure 2. In the left and center panels show the data available from the MWR and RWP, respectively. The right panel presents the intersect of the dates for which both MWR and RWP exist for the same period. Data can be downloaded from http://nycmetnet.ccny.cuny.edu/.

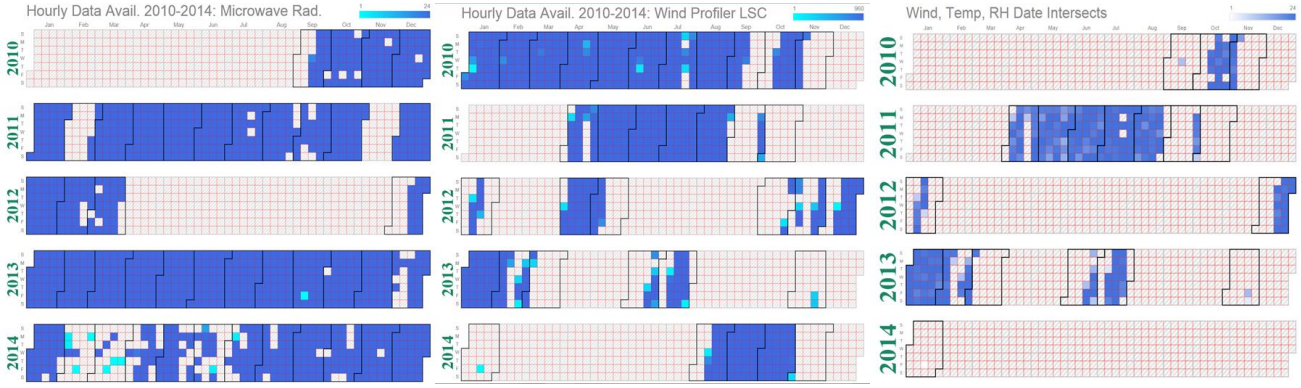

Figure 2: Data availability for the microwave radiometer (left), the radar wind profiler (middle), and the days for which there are concurrent data for the radiometer and wind profiler.

3.3 Static Stability Calculation

In order to create a catalog of the data according to static stability, an averaging process was performed so as to represent a single hour of profile measurements by its static stability. Since the MWR measures values up to a height of 9800m above instrument level (AIL; MWR is located on a rooftop located approximately 60 meters above sea-level). From the climatology of the virtual potential temperature the vertical limit of the average was chosen at 500m since most of the diurnal variability of θ_v is contained below that height.

The microwave radiometer measures all the quantities necessary for the calculation of the virtual potential temperature all as a function of height. The static stability of the atmosphere is an evaluation based solely on the profile of the virtual potential temperature, θ_v (K) which can be calculated by (Stull 1988)

$$\theta_v = \theta\left(1 + 0.61 r_v - r_l\right) \tag{1}$$

where θ, is the potential temperature, r_v is the water vapor mixing ratio, and r_l is the liquid water mixing ratio. The mixing ratios are calculated from the profiles of the water vapor density and the liquid water density measured by the MWR (profiles of these variables are not shown). At each height of a given hour the vertical gradient of $\theta_v(z)$ is calculated using a numerical forward finite difference (Heath 2002),

$$\frac{\partial \theta_v(z_1)}{\partial z} \approx \frac{\Delta\theta}{\Delta z} = \frac{\theta(z_2) - \theta(z_1)}{z_2 - z_1} \tag{2}$$

where $z_2 > z_1$. The criteria for static stability is then based on the sense of this gradient (Arya 2008),

$$\frac{\partial \theta_v}{\partial z}\begin{cases} > 0 & stable \\ = 0 & neutral \\ < 0 & unstable \end{cases} \tag{3}$$

3.6 Boundary Layer Heights

Calculating the boundary layer heights was done using two methods (Seidel, Ao, and Li 2010). The estimation of the boundary layer height was done only for data that extended up to the 2 km range.

1. Potential Temperature Method: The boundary layer height is estimated to be at the location of the maximum vertical gradient of potential temperature: $\max\left(\frac{\partial\theta}{\partial z}\right)$.
2. Relative Humidity Method: The boundary layer height is estimated to be at the location of the minimum vertical gradient of the relative humidity: $\max\left(\frac{\partial(RH)}{\partial z}\right)$.

Both vertical gradients are calculated using a finite difference formulation as in Equation 2.

4. Results

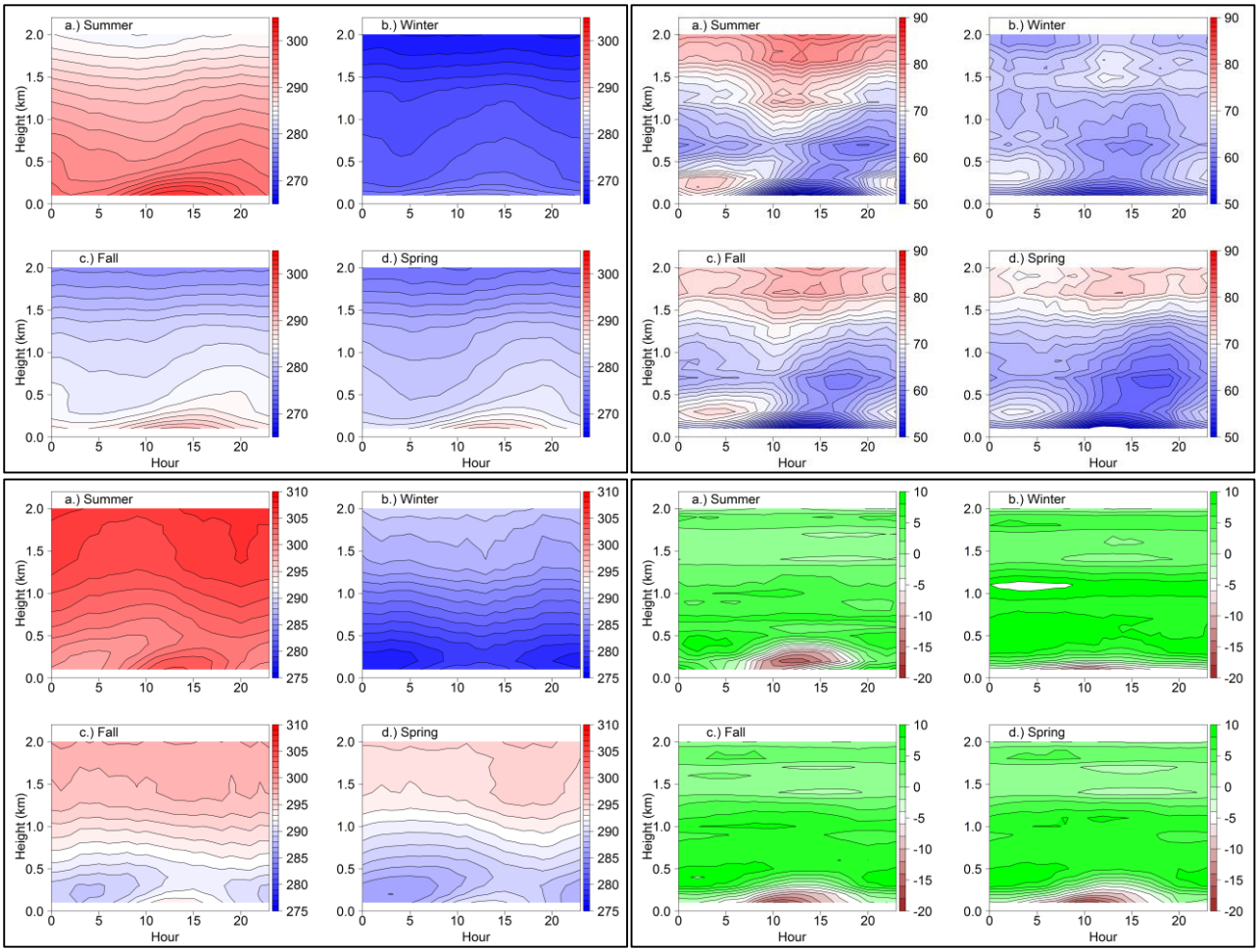

Figure 3: Seasonal diurnal averages from variables measured by the microwave radiometer. Top (left to right): Temperature (K), Relative Humidity (%). Bottom (left to right): Virtual Potential Temperature, θ_v (K), and the vertical gradient of virtual potential temperature ($\partial\theta_v/\partial z$) (K/km).All times are in local time*

In Figure 3, diurnal averages per season for four variables are shown. The data shown in Figure 2 is separated into the summer (June July August), winter (December, January, February), fall (September, October, November) and spring (March, April, May).

The temperature results show a typical pattern as expected for each season, namely, the winter and summer temperatures correspond to the periods of time where the incoming radiation is at a minimum and at a maximum, respectively, and thus exhibit the usual cooling/warming that dominates each period. From these plots it can be seen that the hours of peak insolation occur between the hours of 10:00 and 15:00. Note the sinusoidal pattern formed by the contours of the temperatures in both of these seasons, and looking at the portion with an upward concavity, the winter temperature contours are the only season to have peaks that line up directly on top of each other. A similar pattern can be seen in the relative humidity contours, where a closed-peak which occurs around 0.6 km for every season at around 15:00, with the winter peak closest to this hour and the peaks in other seasons offset to subsequent hours.

The variation in stability conditions are shown in the θ_v and $\partial\theta/\partial z$ contours, with the magnitude represented by the value of the gradient. The hotter θ_v values and corresponding large negative values of $\partial\theta/\partial z$ present in the summer is consistent with the warmer temperatures near the surface that lead to larger instabilities.

In this analysis we wanted to take a look at an hourly time series of the static stability. In Figure 3, the contours of $\partial\theta_v/\partial z$ show great variability of activity up to a height of 500 meters. Taking the average of the values of $\partial\theta_v/\partial z$ up to 500 meters for each hour, and then calculating the diurnal climatology for each season results in the time-series shown in Figure 4. During the peak hours of sunlight, the heating of the surface during the summer causes greater instability than the heating during the winter. The average winter diurnal cycle maintains a near-neutral to stable static stability conditions. Comparing the diurnal average of static stability to the static stability during a heat wave event that occurred July 2013 shows how the intense heating of the surface is later transported to the atmosphere above. Local instability during a heat wave event is more than twice than seasonal summer values. Recent studies have shown that anthropogenic heating may be a significant source of heat in urban locations (Salamanca et al. 2014) . Simulations of a heat wave in 2010 over New York City that seek to quantify the effect of anthropogenic heating on the vertical profile of the atmosphere can be found in the literature (Gutiérrez et al. 2015).

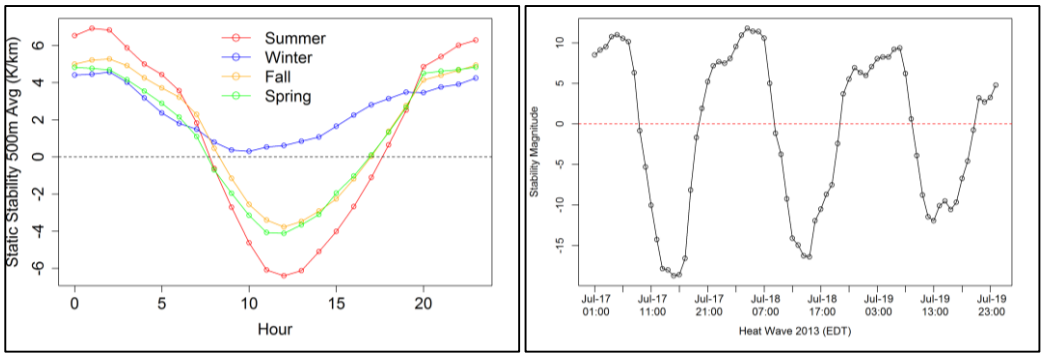

Figure 4: Time series of averaged (up to 500m) local static stability for each season (left) and for the July 2013 heat wave (right).

The instabilities present during the daylight hours is expected to create higher values for the heights of the PBL given the extra energy provided to the rising thermals produced by both solar radiation heating and anthropogenic heating from the built environments. This can be seen in the peak values in Figure 5 of the PBLH that occur midday across all seasons. Although it is expected that greater heights would occur during the summer season, the results in the figure show higher values in the winter using the humidity method. However similar results are found in the for the city of Oakland, California in which the winter seasons show greater values of the PBLH for the winter and smaller values during the summer (Seidel, Ao, and Li 2010).

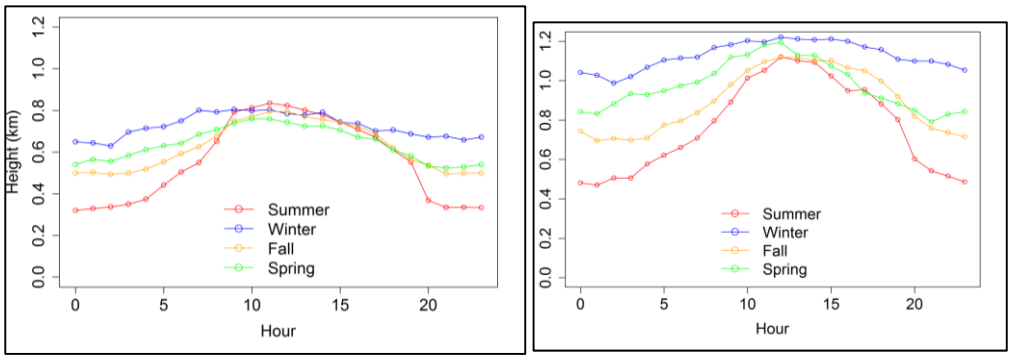

Figure 5: Seasonal diurnal average of the boundary layer height as calculated using the Potential Temperature method (left) and the Relative Humidity method (right).

Finally, horizontal momentum profiles, measured by the radar wind profiler, are shown in Figure 6. Low wind speeds in the lower levels dominate the majority of the midday and afternoon periods, while the winter experiences more shearing in the lower levels. The wind directions for all seasons experience low level southeast wind which turn towards the northwest with increasing height. The downward vertical wind speeds (not shown) mostly present in the upper levels winter months may explain why the time evolution of the PBLH is shows only a small change in height throughout the diurnal cycle when compared to the other seasons. Upward vertical wind speeds due to increased convective activity during the summer, spring, and fall seasons may contribute to the more pronounced bell-shaped curve of the PBL throughout the day.

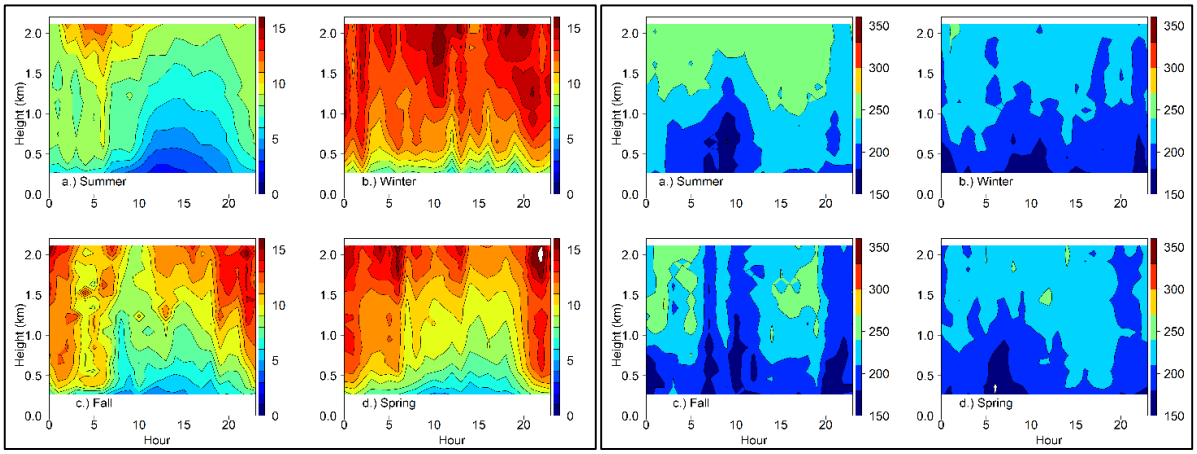

Figure 6: Seasonal diurnal climatology of the horizontal wind speed in m/s (left) and the wind direction in degrees from the north (right).

5. Conclusions and Future Works

Diurnal climatologies were presented of weather variables derived from the output of two surface-based remote sensing instruments in the very dense urban center of New York City. These profiles can help to give a baseline of a typical urban diurnal cycle. The summer months show an increased amount of instability given by the height distribution of the vertical gradient of virtual potential temperature throughout its diurnal profile. This is further seen in the time-series profile of its 500m average, where the winter experiences a minimum near-neutral static stability whereas the summer has a maximum static stability of -6 K/km. Comparison of these diurnal climatologies can also be used to classify heat events by their static stability, as shown with the July 2013 case.

Future work will focus on inclusion of other observation instruments and in comparison to numerical models. Turbulence profiles will be estimated compared to urbanized-WRF outputs. Analyzing variables such as the Richardson number presents a challenge since the instruments are not co-located. Calculations where the momentum and thermal contributions are combined may be most relevant only in conditions that exhibit similar synoptic conditions for both locations. The careful consideration of these special cases, taking into account both the momentum and thermal measurements, will help in the cataloging of events that can be used to evaluate models for unstable, stable, and near-neutral conditions within urban centers. Future analyses of the atmosphere will also be conducted through the co-operation of a vertically pointing Doppler that is collocated with the radiometer at CCNY.

6. Acknowledgment

This study was made possible through the National Oceanic and Atmospheric Administration – Cooperative Remote Sensing Science and Technology Center (NOAA-CREST). NOAA CREST - Cooperative Agreement No: NA11SEC4810004.

7. References

Arya S. Pal, 2008: *Introduction to Micrometeorology*. 2. ed. International Geophysics Series 79. San Diego, Calif.: Acad. Press.

Chen Fei, Kusaka Hiroyuki, Bornstein Robert, Ching Jason, Grimmond C. S. B., Grossman-Clarke Susanne, Loridan Thomas, et al., 2011: The Integrated WRF/urban Modelling System: Development, Evaluation, and Applications to Urban Environmental Problems. *International Journal of Climatology*, **31 (2)**, 273–88.

Cohn Stephen A., and Angevine Wayne M., 2000: Boundary Layer Height and Entrainment Zone Thickness Measured by Lidars and Wind-Profiling Radars. *Journal of Applied Meteorology*, **39 (8)**, 1233–47.

Emeis Stefan, 2011: *Surface-Based Remote Sensing of the Atmospheric Boundary Layer*. Atmospheric and Oceanographic Sciences Library 40. Dordrecht: Springer.

Gedzelman S. D., Austin S., Cermak R., Stefano N., Partridge S., Quesenberry S., and Robinson D. A., 2003: Mesoscale Aspects of the Urban Heat Island around New York City. *Theoretical and Applied Climatology*, **75 (1-2)**, 29–42.

Gutiérrez Estatio, González Jorge E., Martilli Alberto, Bornstein Robert, and Arend Mark, 2015: Simulations of a Heat-Wave Event in New York City Using a Multilayer Urban Parameterization. *Journal of Applied Meteorology and Climatology*, **54 (2)**, 283–301.

Heath Michael T., 2002: *Scientific Computing: An Introductory Survey*. 2nd ed. Boston: McGraw-Hill.

Martilli Alberto, Clappier Alain, and Rotach Mathias W, 2002: An Urban Surface Exchange Parameterisation for Mesoscale Models. *Boundary-Layer Meteorology*, **104 (2)**, 261–304.

Niyogi Dev, Pyle Patrick, Lei Ming, Arya S. Pal, Kishtawal Chandra M., Shepherd Marshall, Chen Fei, and Wolfe Brian, 2011: Urban Modification of Thunderstorms: An Observational Storm Climatology and Model Case Study for the Indianapolis Urban Region *. *Journal of Applied Meteorology and Climatology*, **50 (5)**, 1129–44.

Oke T. R., 1988: *Boundary Layer Climates*. 2. ed., reprinted. London: Routledge.

Salamanca F., Georgescu M., Mahalov A., Moustaoui M., and Wang M., 2014: Anthropogenic Heating of the Urban Environment due to Air Conditioning: Anthropogenic Heating due to AC. *Journal of Geophysical Research: Atmospheres*, **119 (10)**, 5949–65.

Schmid Paul, and Niyogi Dev, 2012: A Method for Estimating Planetary Boundary Layer Heights and Its Application over the ARM Southern Great Plains Site. *Journal of Atmospheric and Oceanic Technology*, **29 (3)**, 316–22.

Seidel Dian J., Ao Chi O., and Li Kun, 2010: Estimating Climatological Planetary Boundary Layer Heights from Radiosonde Observations: Comparison of Methods and Uncertainty Analysis. *Journal of Geophysical Research: Atmospheres*, **115 (D16)**, D16113.

Stull Roland B., 1988: *An Introduction to Boundary Layer Meteorology*. Atmospheric Sciences Library. Dordrecht ; Boston: Kluwer Academic Publishers.

———, 1991: Static Stability—An Update. *Bulletin of the American Meteorological Society*, **72 (10)**, 1521–29.

Tibana Yehisson, Gutierrez Estatio, Marte Sashary, and Gonzalez J. E., 2014: Modeling Building HVAC Energy Consumption During an Extreme Heat Event in a Dense Urban Environment. In , V002T06A002. ASME.